ChemComm

Cite this: *Chem. Commun.*, 2012, **48**, 11516–11518

www.rsc.org/chemcomm

COMMUNICATION

Copolymer-templated nitrogen-enriched porous nanocarbons for CO_2 capture†

Mingjiang Zhong,[ab] Sittichai Natesakhawat,[bc] John P. Baltrus,[b] David Luebke,[b] Hunaid Nulwala,*[ab] Krzysztof Matyjaszewski*[ab] and Tomasz Kowalewski*[a]

Received 13th September 2012, Accepted 10th October 2012
DOI: 10.1039/c2cc36652e

Nitrogen-enriched porous carbon materials made *via* the carbonization of polyacrylonitrile containing block copolymer act as efficient and highly selective CO_2 sorbents. Nitrogen content and surface area, which are both influenced by pyrolysis temperature and atmosphere, are crucial for CO_2 adsorption performance.

The need to mitigate green-house gas emissions opens the demand for the development of efficient materials for CO_2 capture and storage.[1] Conventional CO_2 capture systems based on chemical absorption through amines have major drawbacks such as large energy consumption and poor material stability. To address these drawbacks, there is a need to develop new materials that should be inexpensive and easily synthesized while possessing high CO_2 adsorption capacity and selectivity, fast adsorption/desorption kinetics, as well as improved thermal stability and resistance to moisture. Various porous solids including zeolites, metal–organic frameworks, covalent organic frameworks, polymers, and nanocarbons have been investigated to date.[1–2] Among them, porous carbons are of particular interest, given their low cost, simple fabrication and high thermal stability.[2g,h] While the straightforward path to enhance the performance of these materials involves tailoring the pore structure, recent results indicate that additional improvement can be achieved through the incorporation of heteroatoms such as nitrogen.[3] Particularly effective way of heteroatom incorporation involves the use of nitrogen-rich precursors such as polyacrylonitrile (PAN).[3a,b] In amine-based sorbents, CO_2 typically reacts with pendant amines yielding carbamate functionality. In contrast, in nitrogen-enriched porous carbons derived from PAN, the active nitrogens are integrated into a partially graphitic network, with "edge functionalities" such as pyridinic, pyridine oxide, pyrrolic and pyridine species expected to play the most active role.[4] This unique feature of such PAN-derived porous carbons holds the promise to significantly decrease the energy consumption for sorbent regeneration. In addition, the robust nature of their cross-linked partially graphitic structure may result in enhanced moisture resistance. Typically, the synthesis of high surface area PAN-based carbon involves an activation step under a CO_2 environment at high temperatures above 900 °C to generate microporosity.[3b,5] However, high temperature treatment is associated with denitrogenation which could adversely affect the capacity and selectivity of CO_2 adsorption. Thus, a milder approach to opening up the porosity of nitrogen-enriched carbons, one which would retain the nitrogen functionalities, would be highly desirable.

We previously developed a simple strategy for synthesizing copolymer-templated nitrogen-enriched porous nanocarbons (CTNCs) which have been successfully used as electrode materials for supercapacitors and electrocatalysts for the oxygen reduction reaction (ORR).[6] Scheme 1 illustrates the simple synthetic route to CTNC starting from the polyacrylonitrile-block-poly(*n*-butyl acrylate) (PAN-*b*-PBA) precursor. The carbonization process involves two steps: (1) thermal annealing-facilitated nanophase separation of block copolymer with simultaneous stabilization of PAN at 280 °C under air; and (2) carbonization of stabilized PAN nanodomains and selective removal of PBA block by thermal treatment at temperatures reaching 500–800 °C under an inert atmosphere. During the first step, the stabilization of PAN is achieved through the partial cross-linking and cyclization of PAN side chains,[7] resulting in a fixed framework desirable for preservation of nanostructure during pyrolysis. The PBA block in the precursor acts as a sacrificial component which generates mesoporosity upon carbonization. The presence of nitrogen heteroatoms in CTNCs leads to the significant enhancement of their performance as electrodes for supercapacitors and facilitates electrocatalytic activity toward the ORR.[6a,b] In the studies reported herein, we explored the potential of CTNCs as sorbents for CO_2 capture, focusing primarily on identifying the "mild" thermal treatment

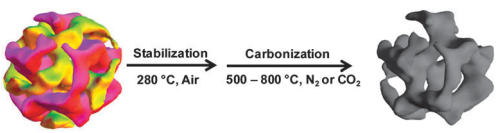

Scheme 1 Synthetic route for CTNC.

[a] *Department of Chemistry, Carnegie Mellon University, 4400 Fifth Avenue, Pittsburgh, Pennsylvania 15213, USA. E-mail: hnulwala@andrew.cmu.edu, km3b@andrew.cmu.edu, tomek@andrew.cmu.edu; Fax: +1-412 929-8102; Tel: +1-412 268-5927*
[b] *National Energy Technology Laboratory, United States Department of Energy, P. O. Box 10940, Pittsburgh, Pennsylvania 15236, USA*
[c] *Department of Chemical and Petroleum Engineering, University of Pittsburgh, Pittsburgh, Pennsylvania 15260, USA*
† Electronic supplementary information (ESI) available: Experimental details and relevant characterization. See DOI: 10.1039/c2cc36652e

conditions which would allow to further increase the surface area without loss of nitrogen functionalities.

The block copolymer precursor with the composition of BA_{76}–AN_{128} and narrow molecular weight distribution (M_w/M_n = 1.18, where M_w and M_n represent the weight and number averaged molecular weights, respectively) was synthesized *via* atom transfer radical polymerization (ATRP) as described in detail elsewhere.[8] Appropriate composition of the block copolymer precursor assures the formation of a bicontinuous morphology which is necessary for good preservation of nanostructure during carbonization[6a] and can be expected to facilitate fast gas transport, desirable in a sorbent material. The stabilized copolymer was carbonized under either nitrogen or CO_2 atmosphere at various pyrolysis temperatures (T_p = 500, 600, 700, and 800 °C). For the convenience of the subsequent discussion, CTNCs made under different conditions will be designated as CTNC-XYYY where X indicates the pyrolysis atmosphere (X = N or C for N_2 or CO_2, respectively) and YYY stands for T_p.

Brunauer–Emmett–Teller (BET) surface areas (S_{BET}) were determined from N_2 adsorption isotherms at 77 K. Surface atomic ratios of nitrogen to carbon (N/C) were measured by X-ray photoelectron spectroscopy (XPS). Table S1 (ESI†) summarizes the characteristics of all carbon samples used in this study.

As shown in Fig. 1a (solid line/squares), for both pyrolysis atmospheres, S_{BET} increased with T_p, with the increase being more pronounced under CO_2. Per our earlier studies, the high surface area of CTNCs can be attributed to two types of pores: (1) mesopores generated by thermal degradation of the PBA phase evidenced by the Bragg peak in small angle X-ray scattering patterns and a hysteresis loop in N_2 adsorption–desorption isotherms (Fig. S1 and S2, ESI†); and (2) micropores generated from cross-linking of the PAN chains and burn-off of amorphous carbon fraction. Such hierarchically porous structure was also evident in transmission electron microscopy images (Fig. S3, ESI†). The micropore surface area (S_{micro}) was obtained from a *t*-plot method using the de Bore equation.[9] Evolution of the surface area due to S_{micro} and mesopore surface area (S_{meso}), is shown in Fig. 1a, with traces marked with circles and triangles, respectively. For pyrolysis under nitrogen (red traces), S_{meso} remained constant throughout the whole temperature range, and the modest increase in the total surface area could be accounted for by the modest increase of S_{micro}. For $T_p \leq 700$ °C the main effect due to CO_2 atmosphere was in the measurably higher value of S_{meso}, which could be interpreted as the evidence of "mild" reactivity toward carbon matrix, resulting in opening up of some occluded mesopores. The situation changed dramatically at T_p = 800 °C, with pyrolysis under CO_2, leading to over a threefold increase of S_{micro}. Changes in S_{BET} with T_p were paralleled by the decrease of N/C ratio (Fig. 1b). As expected, carbonization under CO_2 yielded CTNC-C materials with lower nitrogen content compared to CTNC-N formed at the same T_p. However, for $T_p \leq 700$ °C this lowering was mild and did not exceed 16%. As the pyrolysis temperature was further increased to 800 °C under CO_2, the N/C ratio dropped sharply approximately by 40%. Coincidence of this sharp drop in nitrogen content with the extensive formation of micropores strongly suggests that the nitrogen loss is associated with the burn-off of the amorphous fraction of the material.

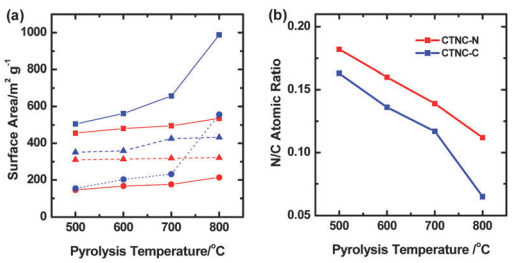

Fig. 1 (a) Effect of T_p on surface area (red: CTNC-N; blue: CTNC-C; solid line-squares: S_{BET}; dot line-circles: S_{micro}; dash line-triangles: S_{meso}); (b) Effect of T_p on N/C atomic ratio.

CO_2 adsorption measurements revealed that CTNCs prepared under both atmospheres acted as efficient CO_2 sorbents, reaching CO_2 capacities comparable to other carbon-based materials.[3b–e,5] Adsorption isotherms of the samples with the highest surface area in both series (CTNC-N800 and CTNC-C800) are shown in Fig. 2a and b. Results for the samples pyrolyzed at all temperatures are also shown in Fig. 2c as plots of ambient pressure adsorption capacity *vs.* T_p for measurements carried out at room temperature and at 0 °C. In all cases, CO_2 adsorption capacity increased with the increase of pyrolysis temperature and was higher for samples pyrolyzed under CO_2, pointing to the importance of surface area of materials, which also increased in the similar order. The dependence on surface area became particularly clear when plotting the results as "geometric adsorption capacity" (adsorption capacity per unit surface area), as shown in Fig. 2d. In these plots, the geometric adsorption capacity of CTNC-N remained independent of T_p, indicating that the surface properties of the pores forming under those conditions remained the same. Geometric adsorption capacities of CTNC-Cs pyrolyzed at temperature in the range of 500–700 °C were comparable to those for CTNC-Ns, and were similarly insensitive to the T_p, taking a sharp drop for pyrolysis at 800 °C. This result is of particular interest, since it indicates that micropores, which formed extensively in this

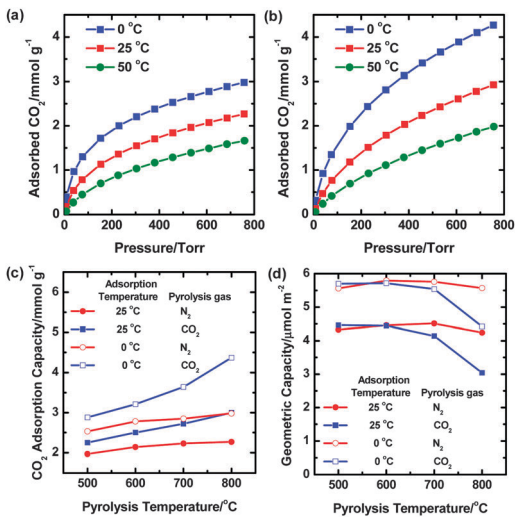

Fig. 2 (a) CO_2 adsorption isotherm of CTNC-N800; (b) CO_2 adsorption isotherm of CTNC-C800; (c) Effect of T_p on CO_2 adsorption capacity of CTNCs (0 and 25 °C, ambient pressure); (d) Effect of T_p on CO_2 adsorption capacity per unit surface area (0 and 25 °C, ambient pressure).

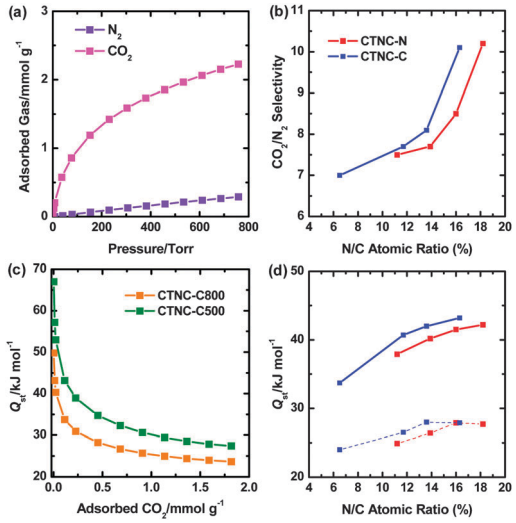

Fig. 3 (a) Comparison of 25 °C adsorption isotherms of CO_2 and N_2 for CTNC-N700; (b) Correlation between CO_2/N_2 selectivity and N/C atomic ratio; (c) Isosteric heats of CO_2 adsorption (Q_{st}) by CTNC-C500 and CTNC-C800; (d) Correlation between Q_{st} and N/C atomic ratio at different CO_2 coverages (red: CTNC-N; blue: CTNC-C; solid line: 0.1 mmol g^{-1} of CO_2 adsorbed; dash line: 1.8 mmol g^{-1} of CO_2 adsorbed).

temperature range under CO_2 and were responsible for the marked increase of the surface area, contributed less to the overall CO_2 adsorption capacity. It is noteworthy that, as discussed earlier, this drop of geometric adsorption capacity has been found to correlate with the sharp decrease of N/C ratio observed for CNTC-C800.

Further indications of the critical importance of nitrogen heteroatoms came from the assessment of adsorption selectivity, carried out by comparing room temperature adsorption isotherms of CO_2 with those obtained in the separate experiments for N_2 (Fig. 3a and b). CTNC-N800 and all other materials exhibited good selectivity for CO_2 manifested by 7 to 10 fold larger amount of adsorbed CO_2 over N_2. The CO_2/N_2 selectivity, calculated as a molar ratio of CO_2 and N_2 adsorbed at 760 Torr, turned out to be strongly favoured by a higher nitrogen content. Similar conclusions about the role of surface nitrogens can be drawn from the analysis of isosteric heats of CO_2 adsorption (Q_{st}), calculated from the slopes of isosteres which were constructed from the predicted saturation coverages using the Langmuir–Freundlich equation (Fig. 3c and d).[10] The characteristic initial sharp decrease to the plateau observed in these curves (Fig. 3c) is likely indicative of initial adsorption driven by more active nitrogen surface sites. Additional evidence of the importance of nitrogen sites comes from the clear decrease of Q_{st} with the decrease of N/C ratio (Fig. 3d). For a higher CO_2 coverage (dash line traces in Fig. 3d), the dependence of Q_{st} at higher N/C ratio was much less pronounced. As shown in Fig. 3b and d, for any given nitrogen content CTNC-Cs exhibited higher selectivity and Q_{st} than CTNC-Ns. This may be the evidence of the ability of CO_2 treatment to more effectively expose nitrogen functionalities on the surface by removal of amorphous carbon and by generation of micropores.

In conclusion, we have demonstrated that nitrogen-enriched porous nanocarbons prepared by pyrolysis of block copolymers containing PAN are promising candidates for CO_2 capture, as they show not only high adsorption capacity but also good CO_2 selectivity over N_2. The adsorption capacity can be increased by enlarging the surface area under CO_2 treatment at temperatures not exceeding 700 °C. While CO_2 treatment at a higher temperature of 800 °C produced even more significant increase of surface area and CO_2 capacity, it came at the expense of reduced selectivity, presumably caused by the loss of nitrogen. These results point to the need of balancing the N/C ratio and high surface area in optimization of CTNC materials for selective CO_2 capture. One can envision that the desirable increase of surface area and decrease of pore size could be achieved without compromising the nitrogen functionality by reducing the size of the sacrificial block. The primary challenge with adopting such strategy would be to overcome the concomitant decrease of thermal stability of block copolymer nanostructure.

Financial support was provided by the National Science Foundation (DMR-0304508 and DMR 09-69301, and DMR-0936384 for Cornell High Energy Synchrotron Source), and CRP Consortium at Carnegie Mellon University. This technical effort was also performed in support of U.S. Department of Energy's National Energy Technology Laboratory's on-going research on CO_2 capture under the contract DE-FE0004000.

Notes and references

1 (*a*) D. M. D'Alessandro, B. Smit and J. R. Long, *Angew. Chem., Int. Ed.*, 2010, **49**, 6058; (*b*) K. S. Lackner, *Science*, 2003, **300**, 1677.
2 (*a*) A. Zukal, I. Dominguez, J. Mayerova and J. Cejka, *Langmuir*, 2009, **25**, 10314; (*b*) O. K. Farha and J. T. Hupp, *Acc. Chem. Res.*, 2010, **43**, 1166; (*c*) H. Furukawa and O. M. Yaghi, *J. Am. Chem. Soc.*, 2009, **131**, 8875; (*d*) D. Wu, F. Xu, B. Sun, R. Fu, H. He and K. Matyjaszewski, *Chem. Rev.*, 2012, **112**, 3959; (*e*) G. T. Rochelle, *Science*, 2009, **325**, 1652; (*f*) L. Wang and R. T. Yang, *J. Phys. Chem. C*, 2011, **116**, 1099; (*g*) C. Liang, Z. Li and S. Dai, *Angew. Chem., Int. Ed.*, 2008, **47**, 3696; (*h*) J. Lee, J. Kim and T. Hyeon, *Adv. Mater.*, 2006, **18**, 2073.
3 (*a*) M. Nandi, K. Okada, A. Dutta, A. Bhaumik, J. Maruyama, D. Derks and H. Uyama, *Chem. Commun.*, 2012, **48**, 10283; (*b*) W. Shen, S. Zhang, Y. He, J. Li and W. Fan, *J. Mater. Chem.*, 2011, **21**, 14036; (*c*) G.-P. Hao, W.-C. Li, D. Qian and A.-H. Lu, *Adv. Mater.*, 2010, **22**, 853; (*d*) M. Sevilla, P. Valle-Vigon and A. B. Fuertes, *Adv. Funct. Mater.*, 2011, **21**, 2781; (*e*) Q. Li, J. Yang, D. Feng, Z. Wu, Q. Wu, S. Park, C.-S. Ha and D. Zhao, *Nano Res.*, 2010, **3**, 632.
4 J. R. Pels, F. Kapteijn, J. A. Moulijn, Q. Zhu and K. M. Thomas, *Carbon*, 1995, **33**, 1641.
5 M. Nandi, K. Okada, A. Dutta, A. Bhaumik, J. Maruyama, D. Derks and H. Uyama, *Chem. Commun*, 2012, **48**, 10283.
6 (*a*) M. Zhong, E. K. Kim, J. P. McGann, S.-E. Chun, J. F. Whitacre, M. Jaroniec, K. Matyjaszewski and T. Kowalewski, *J. Am. Chem. Soc.*, 2012, **134**, 14846; (*b*) J. P. McGann, M. Zhong, E. K. Kim, S. Natesakhawat, M. Jaroniec, J. F. Whitacre, K. Matyjaszewski and T. Kowalewski, *Macromol. Chem. Phys.*, 2012, **213**, 1078; (*c*) T. Kowalewski, N. V. Tsarevsky and K. Matyjaszewski, *J. Am. Chem. Soc.*, 2002, **124**, 10632.
7 E. Fitzer, *Carbon*, 1989, **27**, 621.
8 (*a*) C. Tang, B. Dufour, T. Kowalewski and K. Matyjaszewski, *Macromolecules*, 2007, **40**, 6199; (*b*) C. B. Tang, T. Kowalewski and K. Matyjaszewski, *Macromolecules*, 2003, **36**, 1465; (*c*) K. Matyjaszewski, *Macromolecules*, 2012, **45**, 4015; (*d*) K. Matyjaszewski and J. Xia, *Chem. Rev.*, 2001, **101**, 2921.
9 J. H. Deboer, B. C. Lippens, B. G. Linsen, Jc. Broekhof, A. Vandenhe and T. J. Osinga, *J. Colloid Interface Sci.*, 1966, **21**, 405.
10 S. Natesakhawat, J. T. Culp, C. Matranga and B. Bockrath, *J. Phys. Chem. C*, 2006, **111**, 1055.

